--- Chapter 2 ---

Grueneberg ganglion olfactory subsystem employs a cGMP signaling pathway

Cambrian Y. Liu, Scott E. Fraser, David S. Koos

This chapter is reproduced with minor modification from

> Liu CY, Fraser SE, and Koos DS. Grueneberg ganglion olfactory subsystem employs a cGMP signaling pathway. *J Comp Neurol* 516: 36-48, 2009.

D.S.K. collected the data and images that were used in Figure 7.

ABSTRACT

The mammalian olfactory sense employs several olfactory subsystems situated at characteristic locations in the nasal cavity to detect and report on different classes of odors. These olfactory subsystems use different neuronal signal transduction pathways, receptor expression repertoires, and axonal projection targets. The Grueneberg Ganglion (GG) is a newly appreciated olfactory subsystem with receptor neurons located just inside of the nostrils that project axons to a unique domain of interconnected glomeruli in the caudal olfactory bulb. It is not well understood how the GG relates to other olfactory subsystems in contributing to the olfactory sense. Furthermore, the range of chemoreceptors and the signal transduction cascade utilized by the GG have remained mysterious. To resolve these unknowns, we explored the molecular relationship between the GG and the GC-D neurons, another olfactory subsystem that innervates similarly interconnected glomeruli in the same bulbar region. We found that mouse GG neurons express the cGMP-associated signaling proteins phosphodiesterase 2a, cGMP-dependent kinase II, and cyclic nucleotide gated channel subunit A3 coupled to a chemoreceptor repertoire of cilia-localized particulate guanylate cyclases (pGC-G and pGC-A). The primary cGMP signaling pathway of the GG is shared with the GC-D neurons, unifying their target glomeruli as a unique center of olfactory cGMP signal transduction. However, the distinct chemoreceptor repertoire in the GG suggests that the GG is an independent olfactory subsystem. This subsystem is well suited to detect a unique set of odors and to mediate behaviors that remained intact in previous olfactory perturbations.

KEYWORDS

necklace glomeruli, interconnected glomeruli, cGMP, guanylate cyclase, cilia, nasal vestibule, sensory subsystems

INTRODUCTION

Mice and other macrosmatic mammals possess a diverse set of odor-sensing neuronal subsystems that function together to produce a powerful and nuanced sense of smell (Fig. 1A). These subsystems have characteristic locations in the nasal cavity. Each olfactory subsystem utilizes a specific type of chemoreceptor and signal transduction cascade to detect distinct classes of chemicals and ultimately to influence certain behaviors. Once activated, the primary sensory neurons of a given subsystem directly transmit olfactory information to discrete subsystem-specific domains of the first olfactory processing center in the brain, the olfactory bulb. The olfactory subsystems range from being very large and detecting a broad spectrum of chemicals (*e.g.*, volatile molecules distinguished by >1000 odorant receptors on millions of neurons in the mouse Main Olfactory System and Septal Organ) to being very small (*e.g.*, ~550 neurons in the mouse Grueneberg Ganglion) and possessing highly specialized detection functions (*e.g.*, volatile amines detected by trace-amine associated receptor-expressing neurons) (Breer et al., 2006; Munger et al., 2008).

The Main Olfactory System (MOS) is the largest olfactory subsystem and is composed of the odorant receptor-expressing olfactory sensory neurons located within the main olfactory epithelium (MOE). Binding of volatile odor ligands to odorant receptors localized to the cilia of the olfactory sensory neurons triggers the production of cAMP. These transient elevations of cAMP open a cyclic nucleotide gated channel and result in the depolarization of the neurons. The signals are then transmitted along axons to glomeruli in the main olfactory bulb. Another olfactory subsystem, the Accessory Olfactory System (AOS), located in the vomeronasal organ (VNO) in the mouse, is believed to sense pheromones and genetically encoded ligands through a separate set of receptors coupled to cAMP-independent IP_3/PLC signaling cascades. Olfactory inputs from this subsystem are transmitted to the accessory olfactory bulb (Firestein, 2001; Munger et al., 2008). The AOS is involved in behaviors linked to gender identification (Stowers et al., 2002), mating, and aggression (Halpern, 1987) in rodents.

The sensed odorants, mediated behaviors, and signal transduction mechanisms are far less known for the Grueneberg Ganglion (GG), a newly appreciated olfactory subsystem located at the rostral tip of

the rodent nose just inside of the nostrils (Fig. 1A,B). The GG olfactory subsystem consists of a clustered collection of neurons lining the dorsal medial nasal vestibule that are separated from the nasal cavity by a keratinized epithelium (Fig. 1C). This epithelium is permeable to externally applied water-soluble dyes (Brechbuhl et al., 2008), suggesting that the GG may have access to external odors. GG neurons are ensheathed by glial-like satellite cells (Fig. 1D) (Brechbuhl et al., 2008; Grüneberg, 1973; Tachibana et al., 1990). Despite its unusual location and morphology, the olfactory nature of the GG was revealed by its lifelong expression of olfactory marker protein (OMP), a protein that is expressed at varying levels in all of the known olfactory subsystems, as well as its direct innervation of a spatially distinct region of the olfactory bulb at the junction of the main and accessory olfactory bulbs (Fleischer et al., 2006a; Fuss et al., 2005; Koos and Fraser, 2005; Roppolo et al., 2006; Storan and Key, 2006). The GG axons form unusual glomeruli interconnected by axons, and thus appear like beads on a string. The GG glomeruli are very similar in location and morphology to the previously characterized necklace glomeruli (Shinoda et al., 1993; Shinoda et al., 1989), which are formed by the axons of the GC-D olfactory subsystem (Hu et al., 2007; Juilfs et al., 1997; Leinders-Zufall et al., 2007). The olfactory necklace glomeruli are marked by acetylcholinesterase activity and are labeled by an antibody raised against human placental antigen (Shinoda et al., 1993; Shinoda et al., 1989). The GG glomeruli appear immunohistochemically distinct from the necklace glomeruli. However, because of their juxtaposition and similar morphology, we term the interconnected "necklace-like" glomeruli formed by the GG the "necklace-like domain."

The GG forms before birth and persists throughout the animal's entire life (Fleischer et al., 2006a; Fuss et al., 2005; Grüneberg, 1973; Koos and Fraser, 2005; Roppolo et al., 2006; Storan and Key, 2006). Although the GG is present in most mammals (Grüneberg, 1973), its relationship to other olfactory subsystems in contributing to the mammalian olfactory sense is not well understood. As a result, the functional relevance of the GG has remained mysterious.

A recent report suggests that the GG is necessary for mediating a panic-like freezing behavior in adult mice in response to alarm pheromone, a water-soluble but unidentified odor released by animals under stress conditions (Brechbuhl et al., 2008). How the adult GG detects these important odorants is

unclear. Small subsets of GG neurons have been reported to express a variety of chemosensory receptors such as odorant receptors, pheromone receptors, and trace amine associated receptors (Fleischer et al., 2006b; Fleischer et al., 2007); however, such expressions are transient, restricted to fetal and perinatal stages of life. The significance of this transient expression remains unclear because the associated signal transduction molecules, such as G_{olf} and transient receptor potential C2 (TRPC2), canonically employed by these receptors appear not to be expressed (Roppolo et al., 2006).

The anatomical similarity of the necklace and necklace-like glomeruli, as well as the molecular differences between the GG, MOS, and AOS, prompted us to test the GG's relationship to the sensory neurons that innervate the necklace domain, the GC-D olfactory subsystem. The sensory cells in this small but specialized olfactory chemosensory subsystem express a membrane-bound guanylate cyclase (pGC-D) and employ a cGMP signal transduction pathway (Fulle et al., 1995; Juilfs et al., 1997; Leinders-Zufall et al., 2007; Meyer et al., 2000). Like the adult GG, they lack the chemosensory receptors and signal transduction molecules employed by the MOS and AOS (Juilfs et al., 1997; Meyer et al., 2000; Walz et al., 2007). In performing this comparison, we find that the GG employs a cGMP signal transduction system somewhat similar to the GC-D olfactory subsystem; however, the neurons of the GG express a different set of membrane-bound guanylate cyclases throughout the life of the animal. We propose that these receptors mediate the chemosensory function of the GG.

MATERIALS AND METHODS

Animals

Mice were maintained as per Caltech IACUC-approved protocol. Genetically modified mice strains used were 1) OMP-GFP (Potter et al., 2001), 2) GCD-iTG (Hu et al., 2007), 3) GCD-iTL (Walz et al., 2007), and 4) PLP-GFP (Fuss et al., 2000). OMP-GFP mice were generated via a knock-out/knock-in procedure in which the OMP coding region was replaced with GFP by homologous recombination at the *OMP* locus. The resulting mouse strain expresses GFP from the endogenous *OMP* promoter (Potter et al., 2001). GCD-iTG and GCD-iTL mice were generated by the targeted insertion of an internal ribosome

entry sequence (IRES) followed by the tau microtubule localization sequence fused to GFP (GCD-iTG) or LacZ (GCD-iTL) downstream of the endogenous pGC-D coding region, in the *Gucy2d* locus. As a result, transcription from the endogenous *Gucy2d* promoter results in a bicistronic mRNA which is translated into the endogenous pGC-D and a microtubule-localized reporter protein (Walz et al., 2007). PLP-GFP (proteolipid protein-GFP) mice were generated by pronuclear injection of a construct containing a modified 2.4 kb upstream promoter, exon 1, and intron 1of PLP and where subsequent exons were replaced with GFP coding sequence (Fuss et al., 2000; Wight et al., 1993). The resulting transgenic mice express endogenous PLP from the unmodified endogenous *PLP* promoter and express GFP from the randomly-inserted, modified, exogenous *PLP* promoter construct (Fuss et al., 2000).

All animals used were postnatal. Immunohistochemical experiments performed in this study to validate these transgenic lines are described in the Results section. Experiments to validate OMP-GFP mice were performed on heterozygous animals that possessed a wild-type allele of OMP.

Immunohistochemistry

Young and adult animals were euthanized with CO_2 and decapitated. Isolated nasal vestibules and other olfactory organs were immersion-fixed in 4% paraformaldehyde in phosphate buffered saline (PBS) overnight at 4˚C. Tissues were decalcified in 13% EDTA overnight. From these preparations, either cryosections (18 μm), thick agarose-embedded sections (100 μm), or whole-mount nasal epithelia were extracted.

Tissue was placed in blocking solution consisting of 0.3% Triton-X in PBS with 4% normal goat or horse serum for >4 h at room temperature. Tissue was incubated with primary antibody (with Triton-X and serum) overnight at 4˚C. For immune-adsorption studies, primary antibody was incubated with a 100-fold molar excess of antigenic blocking peptide before being added to the tissue. The next day, unbound primary antibody was rinsed away with >4 changes of PBS. Secondary antibody was applied for 2 h at room temperature or overnight at 4˚C. After washing, tertiary label (with Triton-X but no serum) was applied to tissue for 2 h at room temperature.

For antibody stainings with diaminobenzidine (DAB) chromogen development, tissue was washed with 0.3% hydrogen peroxide in PBS before the staining process was started. Signal was revealed with a Ni-enhanced DAB kit (Thermo Scientific) with a development time of 5-12 minutes in the dark. DAB-developed tissue was washed in multiple changes of PBS. Tissue was mounted in 80% glycerol, or dehydrated in ascending ethanol/water series, cleared in xylenes, mounted in Krystalon (EMD Chemicals), and coverslipped.

For fluorescently-labeled tissue, the final PBS washes included 0.2 μM Topro-3 (Invitrogen) as a nuclear stain. Tissue was mounted with Gel-Mount (Biomeda) or PBS and coverslipped.

Immunostainings in the GG were repeated on at least 4 entire ganglia with mice at different ages to verify the staining patterns (each mouse has two Grueneberg Ganglia, one per side).

Immunoblots (Western blots)

Freshly dissected tissues from the eyes, nasal vestibules, MOE, kidneys, and intestines of CO_2-euthanized adult mice were separately homogenized using a pestle in RIPA buffer (150 mM NaCl, 1% Triton-X, 0.5% sodium deoxycholate, 0.1% SDS, 50 mM Tris, pH 8.0) with an EDTA-free protease inhibitor cocktail (Roche). After 2 h of mixing at 4˚C, samples were spun at 12,000 *g*. The supernatant was reserved for immunoblots.

For Tris-glycine SDS-PAGE, protein samples were boiled in Laemmli loading buffer (60 mM Tris, 2% SDS, 10% glycerol, 5% β-mercaptoethanol, 0.01% bromophenol blue, pH 6.8) for 5 minutes before loading into the wells of a discontinuous acrylamide gel system with an 8% resolving gel. MagicMark XP protein standard (Invitrogen) was used as a ladder. Separated proteins were transferred to Amersham Hybond N+ nylon membranes (GE Healthcare) overnight at 22V at 4˚C in transfer buffer (39 mM glycine, 48 mM Tris, 0.037% SDS, 20% methanol).

Membranes were blocked in 5% nonfat dry milk in TBST (125 mM NaCl, 25 mM Tris, 0.1% Tween-20, pH 8.0) and incubated overnight at 4˚C with primary antibodies. After extensive washes in TBST, membranes were incubated for 2 h at room temperature with a horseradish peroxidase-conjugated

goat anti-rabbit secondary antibody (Jackson Immunoresearch) at 1:5,000 dilution. Bound antibodies were detected with the Amersham ECL+ enhanced chemiluminescence system (GE Healthcare). Chemiluminescent signal was captured onto X-ray film (Kodak).

Predicted molecular weights were obtained computationally from the protein sequence using the ProtParam program on the Swiss ExPASy Proteomics Server (au.expasy.org). Unless otherwise noted, chemicals were obtained from Sigma.

Antibodies

Primary antibodies used are described in Table 1. For primary antibodies raised in a rabbit, the secondary antibody was biotinylated anti-rabbit IgG, raised in goat (Vector Labs), diluted in saline with normal goat serum at 3 µg/mL working concentration for thin sections, or 0.75 µg/mL working concentration for thick sections or whole mounts. For primary antibodies raised in a goat, the secondary antibody was biotinylated anti-goat IgG, raised in horse (Vector Labs), diluted in saline with normal horse serum at the same concentration used for the anti-rabbit secondary. For fluorescent labeling, tertiary label was streptavidin-conjugated Alexa 555 dye (Invitrogen) at 2 µg/mL working concentration. For DAB-labeling, tertiary label was streptavidin-conjulated horseradish peroxidase (MP Biomedical) at 1:500 working dilution.

The goat anti-OMP antibody used in this study has been validated previously for use on immunoblots and immunohistochemical experiments. Immunoblots of HeLa cells transiently transfected with rat OMP detected a 19 kDa protein corresponding to the molecular weight of OMP and a 38 kDa band that likely represents an OMP homodimer (Koo et al., 2004). In immunostainings performed in mice, this antibody labeled glomeruli in the olfactory bulb and olfactory sensory neurons in the MOE (Cummings et al., 2000). The rabbit anti-GFAP (glial fibrillary acidic protein) antibody used in this study has been used previously in an immunohistochemical study to identify astrocytes in the developing mouse brain (Henion et al., 2003). On immunoblots with rat cerebellum homogenate, this antibody recognized a 50 kDa band corresponding to rodent GFAP and a 45 kDa GFAP-related band (manufacturer's datasheet).

The rabbit anti-PLP (proteolipid protein) antibody has been shown in previous immunohistochemical studies to label specifically myelinated nerve fibers in the mouse (Papastefanaki et al., 2007). The rabbit anti-CNGA3 antibody has been shown previously to recognize a 76 kDa protein corresponding to mouse CNGA3 on immunoblots with mouse retinal homogenate. In immunohistochemical applications, it recognized the anticipated segments on cone photoreceptor neurons. Pre-incubation of the antibody with its antigenic blocking peptide abolished staining on the immunoblots and in the immunofluorescence experiments (Matveev et al., 2008).

Previously unvalidated antibodies were validated in several ways. First, an immunoblot was performed with a lysate of tissue that is known to express the protein of interest. Second, the antibody's suitability for immunohistochemistry was evaluated by fluorescence immunostaining on thin sections of mouse positive control tissue. Third, if the antibody was found to label GG neurons, immunoadsorption studies were performed with an antigenic blocking peptide, when available. Validation experiments performed in this study are described in the Results section.

X-gal histochemistry

The development of X-gal blue precipitate in pGC-D-expressing tissues was performed as previously described (Walz et al., 2007).

Transmission electron microscopy

Mice were anesthetized with Avertin (2-2-2-tribromoethanol, Sigma) and transcardially perfused with fixative (4% paraformaldehyde, 1.25% glutaraldehyde (Ted Pella), in 0.06M phosphate buffer, pH 7.4, 37˚C). Isolated nares were trimmed of excess tissue and post-fixed (4% paraformaldehyde, 1.25% glutaraldehyde, in 0.1M NaCacodylate, pH 7.4, 4˚C). Tissue was stained for 1 h at 4˚C with 2% OsO_4 in veronal acetate + 5% sucrose, washed with 0.1M maleate buffer (pH 5), and incubated for 1 h at room temperature in 1% uranyl acetate prepared in maleate buffer. After dehydration through a graded ethanol series, tissue was embedded in ascending propylene oxide/Epon resin (Fluka) solutions until 100% Epon

resin and solidified at 60˚C. 120 nm semi-serial sections were floated onto formvar-coated copper EM grids (Ted Pella) and allowed to dry; they were then stained with uranyl acetate and lead citrate, rinsed with water, and allowed to dry completely prior to EM imaging.

Optical imaging

Samples were imaged on various Zeiss microscopes depending on the type of staining and the required resolution. Fluorescence imaging was performed on a Zeiss LSM510 upright confocal microscope system. High-magnification (40×, 1.3NA and 63×, 1.25NA oil objectives) fluorescent images were generated from z-projections of approximately 1 µm optical sections by reducing the pinhole size to 1 Airy unit. The pinhole size could be increased to optimize signal-to-noise for weaker signals. Lower-magnification (20×, 0.5NA objective) fluorescence images were assembled from approximately 6 µm optical sections. Multiphoton imaging of PLP-GFP transgenic mice (Fig. 1D) was performed on freshly isolated naris tissue using a 40× water immersion objective and a home-built multiphoton system (Potter et al., 1996). Brightfield images were obtained on a Zeiss Axiophot compound microscope.

Uniform adjustments to image brightness/contrast and noise reduction with a median filter were performed with ImageJ (National Institutes of Health, USA) and Paint Shop Pro (Corel). When comparisons were made between the GG and the MOE, the channel of comparison was imaged with the same power and gain, and subsequent brightness and contrast enhancements were made to the same level in both organs.

RESULTS

Components of the cGMP signaling pathway are expressed in the GG

Phosphodiesterases degrade cyclic nucleotides that are essential second messengers involved in neuronal activation in most olfactory subsystems. To examine phosphodiesterase expression in the GG and other mouse olfactory subsystems, we used a strain of mice (OMP-GFP) to help visualize these

olfactory subsystems in their anatomical locations. In OMP-GFP mice, the primary olfactory sensory neurons of all olfactory subsystems are highlighted by the expression GFP (Potter et al., 2001). Immunostaining these transgenic mice with an OMP-specific antibody revealed that all GFP-expressing neurons were strongly labeled by the antibody (Fig. 1E,F). Antibody labeling was observed in the GFP-positive glomerular layer of the olfactory bulb (Fig. 1G), but labeling was not found in GFP-negative cells in the nasal vestibule, MOE, or olfactory bulb (n = 4 mice). These results show that the OMP-GFP mouse strain faithfully reveals the location of the primary sensory neurons of the mouse olfactory subsystems.

The neurons of the GG do not express the cAMP-specific phosphodiesterase (PDE4A) that is found in the olfactory sensory neurons (OSNs) of the MOS. In neonatal mice, an antibody to the cAMP-selective PDE4A specifically labeled the highly OMP-expressing neurons in the MOE (n = 4; Fig. 2A), consistent with previous reports (Juilfs et al., 1997). In contrast, all OMP-expressing GG neurons were negative for PDE4A (n = 4 ganglia from the same mice as Fig. 2A; Fig. 2B), suggesting that the cAMP signaling pathway commonly used in OSNs is not employed by the GG neurons. On immunoblots with MOE lysate, this antibody recognized five bands between 60 and 100 kDa that likely represent splice variants of PDE4A (Bolger et al., 1996; Rena et al., 2001; Shakur et al., 1995).

In contrast, we find the expression in the GG of the cGMP-stimulated phosphodiesterase 2a (PDE2A) isoform (Bender and Beavo, 2006), which implicates cGMP as the predominant second messenger molecule in this olfactory subsystem, similar to the neurons of the GC-D olfactory subsystem (Juilfs et al., 1997). In the MOE, a PDE2A antibody labeled only a small subset of weakly OMP-expressing neurons in the caudal neuroepitheliary layers (Fig. 2C), corresponding to the GC-D neurons (Ring et al., 1997). The recognized protein was ~100 kDa on immunoblots, close to the predicted 105 kDa size for mouse PDE2A. In the nasal vestibule, OMP-expressing GG neurons were intensely positive for PDE2A from birth to adult-aged mice (Fig. 2D). Vascular endothelial cells were also labeled by the antibody (Sadhu et al., 1999). Pre-incubation of PDE2A antibody with its antigenic peptide, or omission of the primary antibody, abolished the staining (Fig. 2E,F).

cGMP-Dependent Kinases. Downstream signaling effects of cGMP are mediated by cGMP-dependent kinases, which exist in three isoforms, the splice-variants cGKIα and cGKIβ, and cGKII (Feil et al., 2003). A cGKII antibody labeled OMP-expressing GG neurons in the nasal vestibules of adult OMP-GFP mice (Fig. 3A). The labeling appeared to be concentrated on the membranes of GG neurons, consistent with previous descriptions of cGKII localization (Feil et al., 2003). This antibody was validated by its labeling of the brush borders of mouse intestinal villi (Fig. 3B), in accord with previous reports of cGKII protein expression (Golin-Bisello et al., 2005; Jarchau et al., 1994; Markert et al., 1995). On immunoblots with mouse intestinal lysate, this antibody recognized a ~80 kDa protein consistent with the 86 kDa cGKII protein and a ~70 kDa band that may correspond to a previously-observed 72 kDa degradation product of cGKII (El-Husseini et al., 1998; French et al., 1995). Collectively, these results suggest that the cGKII antibody faithfully labels cGKII-expressing cells and that cGKII mediates downstream signaling effects of cGMP production in the GG olfactory subsystem.

Cyclic Nucleotide Gated Channels. In order to further investigate the molecular nature of the GG neurons we explored the expression of cyclic nucleotide gated (CNG) channels that can mediate neuronal depolarization. In the neurons of the MOS, the tetrameric CNG channel composed of two CNGA2, one CNGA4, and one CNGB1b subunits depolarizes the neuron during elevation of cGMP or cAMP levels (Biel and Michalakis, 2007; Frings et al., 1992). Previous work has shown that these channel subunits are not expressed in the GG (Roppolo et al., 2006).

An antibody specific to mouse CNGA3 (Matveev et al., 2008) revealed that the neurons of the GG express CNGA3. The antibody was validated in thin sections from the mouse retina, revealing staining in cone photoreceptors (Fig. 3C), consistent with CNGA3's known role in cGMP-dependent phototransduction as a heterotetramer with CNGB3 (Kohl et al., 1998; Tanaka et al., 1989). In the nasal vestibules of OMP-GFP mice, the antibody specific to CNGA3 labeled unusual whip-like subcellular domains on the somata of OMP-expressing GG neurons (Fig. 3D). Interestingly, the same CNGA3 subunit is expressed on the ciliary receptive domains of the GC-D neurons (Leinders-Zufall et al., 2007; Meyer et al., 2000). GC-D neurons visualized in a *Gucy2d* targeted GFP transgenic mouse line, GCD-iTG

(Hu et al., 2007; Walz et al., 2007), exhibited CNGA3 antibody labeling in their dendritic knobs (Fig. 3E). Thus, CNGA3 is expressed by the neurons of the olfactory subsystems that innervate the necklace and necklace-like domains.

Particulate guanylate cyclase expression in the GG

In the GC-D olfactory subsystem, a particulate guanylate cyclase isoform (pGC-D) is thought to serve as the chemosensor, producing cGMP in response to urinary derivates (guanylin and uroguanylin) (Leinders-Zufall et al., 2007). The sensory neurons of the GC-D olfactory subsystem can be recognized in the neonatal mouse MOE by their staining with a PDE2A antibody; these same neurons were GFP-positive in the GCD-iTG mice (Fig. 4A), verifying the fidelity of GCD-iTG mice in revealing the neurons employing pGC-D. The similar innervation targets of the GG and the GC-D olfactory subsystems motivated us to search for particulate guanylate cyclase isoforms expressed in the GG that could mediate the GG's chemosensory function.

In contrast to the GC-D olfactory subsystem, GG sensory neurons (recognized with the PDE2A antibody) were not GFP-positive in GCD-iTG neonatal mice. Four ganglia were examined in their entirety, and none of the PDE2A-labeled GG neurons exhibited detectable GFP fluorescence (Fig. 4B). Identical results were obtained in adult (6 weeks old) GCD-iTG mice (n = 6 ganglia) and in a separate *Gucy2d*-targeted, LacZ-expressing transgenic mouse strain (GCD-iTL, n = 4 ganglia). Thus, the GG does not express the pGC-D receptor protein, in contrast to the neurons of the GC-D olfactory subsystem.

In addition to pGC-D, there are six known pGC isoforms in the mouse (A, B, C, E, F, G), each with distinct expression patterns throughout the body, but not yet explored in the olfactory pathway (Kuhn, 2003). A panel of affinity-purified pGC antibodies was used to survey the expression of these other mouse pGCs in the GG. The antibodies to pGC-A, B, C, E, and F were found suitable for use in immunohistochemistry because they labeled the expected cellular structures in the kidney, vasculature, intestine, and eye (pGC-E and pGC-F), respectively, in fluorescent immunostainings (Supporting Fig. 1). Immunoblots performed on the respective tissue lysates confirmed that these antibodies could detect the

proteins of appropriate molecular weights (Table 2). *A priori* control experiments with the pGC-G antibody were not possible because the tissue distribution pattern of this protein in rodents is not fully understood.

Of the six pGC isoforms tested, only antisera directed against pGC-G (Fig. 5A) and pGC-A (Fig. 5B) labeled neurons of the GG. The labeling was entirely absent when these antibodies were pre-incubated with their respective antigenic peptides (Fig. 5C-F). pGC-A is a natriuretic peptide receptor used in a variety of organ systems as a regulator of vascular tone and water retention (Kuhn, 2003). pGC-G is an orphan guanylate cyclase with unknown functions (Kuhn et al., 2004; Schulz et al., 1998). The two isoforms differed in their expression patterns: pGC-G was detected on most GG neurons (Fig. 5A) at both neonatal and adult ages (Fig. 5G,H); in contrast, pGC-A was detected in only a small subset of GG neurons scattered throughout the GG organ (Fig. 5B). In immunoblotting experiments with nasal vestibule lysate, the pGC-G antibody recognized a single ~120 kDa band, consistent with the predicted size of 123 kDa for mouse pGC-G (Fig. 5M). pGC-G expression was absent from the GC-D neurons (n = 5 mice; Fig. 5I,J).

pGC-G is localized to GG cilia

Intriguingly, pGC-G expression was restricted to unusual subcellular domains on the somata of GG neurons, very similar to the pattern of the CNGA3 staining. Thin sections imaged at high magnification revealed that the pGC-G-immunoreactive region appeared as thin fibers on the peripheries of the GG somata, with no observable directional preference. These fibers followed the contours of GG cells in a “whip-like” fashion (Fig. 5K,L). In some cases, the fibers extended from one GG neuron to touch a neighboring GG neuron. However, none of these whip-like fibers protruded from a GG neuron into the nasal cavity (n = 16 ganglia).

Immunoreactivity for pGC-G protein was not detected on the tight-fitting glial cells that ensheath the GG neurons. These ensheathing glia could be visualized in the PLP-GFP mouse line (Fuss et al., 2000), in which the proteolipid protein (PLP) promoter drives the expression of GFP. The ensheathing

glia were not labeled by an antibody raised against PLP protein; this is not surprising given that multiple protein products can be derived from PLP promoter activity (Macklin et al., 1987; Nave et al., 1987). The GFP-expressing cells in PLP-GFP mice were colabeled by an antibody to glial fibrillary acidic protein (Fig. 6A), which has been previously shown to mark the ensheathing glia of GG olfactory subsystem (Brechbuhl et al., 2008). In the PLP-GFP transgenic, GFP-positive glial cells and their processes can be seen to wrap the clusters of GG neurons (Fig. 6B), including the intensely pGC-G stained structures at the periphery of the GG somata (Fig. 6C).

Electron Microscopy. To identify the GG subcellular domains that are decorated with pGC-G, we performed an ultrastructural analysis of the ganglion using transmission electron microscopy. In semi-serial thin sections of the adult nasal vestibule, each GG neuron was observed to be decorated by a plurum of cilia whose ultrastructural morphologies are consistent with the pGC-G-labeled subcellular domains seen with light microscopy. These cilia are seen erupting out from clusters of basal bodies deep within the cell soma (Fig. 7A,B). The cilia are grouped (Fig. 7C,D) and appear as long bundles that follow the contour of the cell in a variety of orientations (Fig. 7E,F). The encasement of GG neurons by the ensheathing cells was tight enough that the ciliary bundles were observed to be partially indented into the membranes of the GG cells. Ciliary bundles were not observed to protrude through this ensheathing cell layer, nor were ganglionic processes found to project into the nasal cavity.

DISCUSSION

Particulate guanylate cyclase expression in the GG

Two different receptor guanylate cyclases (pGC-G and pGC-A), a cGMP-stimulated phosphodiesterase (PDE2A), a cGMP-dependent kinase (cGKII), and a cGMP-activated channel containing CNGA3 subunits are expressed in the GG. Together, these components, from receptor to effector, reveal a cGMP signal transduction pathway that can mediate GG chemoreception (Fig. 8). The expression of pGC-G on most neurons of the GG and its exclusion from many other tissues in the mouse (Kuhn et al., 2004) suggests that pGC-G is responsible for mediating a GG-specific chemosensory

function. Assuming that they serve as the sole receptors, the ligands for pGC-A and pGC-G dictate the range of molecules that are detected by the GG. These ligands may include natriuretic peptides or the, at-present, chemically undefined mammalian alarm pheromone. Binding of the cognate ligands to pGC-A/G triggers the production of cGMP, subsequently inducing CNGA3 channels to depolarize the GG neuron and activating cGKII kinase activity. PDE2A degrades the cyclic nucleotides, thereby resetting the system to the un-activated state.

It is possible that direct binding of ligands to pGC-G and pGC-A is not the only means of GG chemosensory transduction. There may be unidentified chemoreceptors that act in parallel or upstream of the particulate guanylate cyclases. For example, in the eye, light absorbed by photopigments results in the hydrolysis of cGMP by Pde proteins and subsequent closure of cyclic nucleotide gated channels (Bender and Beavo, 2006; Biel and Michalakis, 2007). Calcium-inhibited particulate guanylate cyclases work downstream to restore the original cGMP levels and thereby to end the hyperpolarizing signal (Sokal et al., 2003). Thus, the guanylate cyclases play a crucial role in the visual system, but they are not directly responsible for the retinal sensitivity to light. While there is ample evidence that pGC-D is the first step in chemosensory transduction in the GC-D olfactory subsystem, recent experiments have suggested a role for adjunctive proteins. Individual neurons of the GC-D olfactory subsystem differ in their responses to the pGC-D ligands uroguanylin and guanylin (Duda and Sharma, 2008; Leinders-Zufall et al., 2007). Moreover, the detection of carbon dioxide (CO_2) by this olfactory subsystem requires a carbonic anhydrase to convert CO_2 into the pGC-D-activating bicarbonate form (Sun et al., 2009). Further biochemical studies on pGC-G will help uncover its exact role in the GG olfactory subsystem.

The localization of pGC-G and pGC-A to GG neuronal cilia suggests a critical contribution of these receptor guanylate cyclases to the chemosensory function of the GG olfactory subsystem. Ciliary localization of chemosensory receptors and signal transduction components is a common feature of the olfactory subsystems. For example, odorant receptors, pheromone receptors, and signaling elements such as adenylyl cyclase, G protein, and cyclic nucleotide gated channels are preferentially localized to cilia in

the MOS or microvilli in the AOS (Firestein, 2001). Similarly, pGC-D is localized to the cilia of neurons in the GC-D olfactory subsystem (Juilfs et al., 1997).

The far-forward location of the GG, just inside of the nostrils, appears to place the GG in prime position to be the first olfactory subsystem to interrogate inhaled molecules. However, in contrast to the receptive ciliary structures of other olfactory subsystems, the GG cilia do not protrude into the nasal cavity. The ultrastructural results of this study generally agree with previous electron microscopic studies on the GG in the mouse (Brechbuhl et al., 2008) and the musk shrew (Tachibana et al., 1990). However, in our studies, no GG cilia were found to escape entrapment by the ensheathing cell population and project into the extra-ganglionic matrix, in contrast to previous reports (Brechbuhl et al., 2008). These results suggest that potential GG ligands must be able to penetrate rapidly both the keratinized epithelium and the ensheathing cell layer to access the cilia. Small gaseous or lipid-soluble molecules are thus candidates for detection by the GG. While GG cilia are decorated with chemoreceptors, their subsurface location suggests that they are not optimally positioned for direct sampling of odorants drawn in the airspace of the nasal cavity. The logic for this unusual subsurface arrangement of GG receptive structures is unclear and should be a continued topic of study.

Classification of the GG olfactory subsystem

The GG should be classified as a noncanonical olfactory subsystem because it employs a cGMP signaling pathway, distinct from the MOS. The far-rostral location, unusual morphology, and unique receptor repertoire of the GG suggest that this olfactory subsystem senses a unique set of odors. The GG shares some signal transduction components with the GC-D olfactory subsystem; however, the GG might be activated differently during various odor sampling modalities such as sniffing (Verhagen et al., 2007), normal smelling, and retronasal flow due to its position and ensheathment.

The similarities in the signal transduction pathways used by the GG and the GC-D neurons extend to their innervation of the necklace and necklace-like domains, suggesting that they form a unique pathway of olfactory information processing. Both the necklace and the necklace-like domains form

distinct sets of interconnected glomeruli (“separate necklaces”) at the junction of the main and accessory olfactory bulbs. While the exact effects of chemosensory processing in this domain on animal behavior are not known, its unique position, morphology, and signaling repertoire suggest that it effects atypical functions. This is reinforced in recent studies in which a surgical ablation of the GG abolished the animal’s freezing response to the presence of alarm pheromone (Brechbuhl et al., 2008). While the functions of the MOS and the AOS have been explored by genetic ablations (Baker et al., 1999; Stowers et al., 2002; Trinh and Storm, 2003), these ablations should not have affected the GG or GC-D olfactory subsystems. Thus, behaviors that remain intact in these knock-out strains may be transduced by the GG and/or GC-D olfactory subsystems. Genetic ablations targeting cGMP signaling components downstream of the particulate guanylate cyclases might serve as experimental animal models to elucidate functions mediated by this domain of interconnected glomeruli.

ACKNOWLEDGMENTS

We wish to thank P. Mombaerts and W.B. Macklin for generously providing us with genetically-modified mouse strains, X.-Q. Ding for kindly donating antibodies, L.A. Trinh and J. Edens for technical assistance, and J.M. Allman for suggestions on the manuscript. This work was supported by the National Institutes of Health (USA), grant RPN2-EY018241

REFERENCES

Baker H, Cummings DM, Munger SD, Margolis JW, Franzen L, Reed RR, Margolis FL. 1999. Targeted deletion of a cyclic nucleotide-gated channel subunit (OCNC1): biochemical and morphological consequences in adult mice. J Neurosci 19(21):9313-9321.

Bender AT, Beavo JA. 2006. Cyclic nucleotide phosphodiesterases: molecular regulation to clinical use. Pharmacol Rev 58(3):488-520.

Biel M, Michalakis S. 2007. Function and dysfunction of CNG channels: insights from channelopathies and mouse models. Mol Neurobiol 35(3):266-277.

Bolger GB, McPhee I, Houslay MD. 1996. Alternative splicing of cAMP-specific phosphodiesterase mRNA transcripts. Characterization of a novel tissue-specific isoform, RNPDE4A8. J Biol Chem 271(2):1065-1071.

Brechbuhl J, Klaey M, Broillet MC. 2008. Grueneberg ganglion cells mediate alarm pheromone detection in mice. Science 321(5892):1092-1095.

Breer H, Fleischer J, Strotmann J. 2006. The sense of smell: multiple olfactory subsystems. Cell Mol Life Sci 63(13):1465-1475.

Cummings DM, Emge DK, Small SL, Margolis FL. 2000. Pattern of olfactory bulb innervation returns after recovery from reversible peripheral deafferentation. J Comp Neurol 421(3):362-373.

Duda T, Sharma RK. 2008. ONE-GC membrane guanylate cyclase, a trimodal odorant signal transducer. Biochem Biophys Res Commun 367(2):440-445.

El-Husseini AE, Bladen C, Williams JA, Reiner PB, Vincent SR. 1998. Nitric oxide regulates cyclic GMP-dependent protein kinase phosphorylation in rat brain. J Neurochem 71(2):676-683.

Feil R, Lohmann SM, de Jonge H, Walter U, Hofmann F. 2003. Cyclic GMP-dependent protein kinases and the cardiovascular system: insights from genetically modified mice. Circ Res 93(10):907-916.

Firestein S. 2001. How the olfactory system makes sense of scents. Nature 413(6852):211-218.

Fleischer J, Hass N, Schwarzenbacher K, Besser S, Breer H. 2006a. A novel population of neuronal cells expressing the olfactory marker protein (OMP) in the anterior/dorsal region of the nasal cavity. Histochem Cell Biol 125(4):337-349.

Fleischer J, Schwarzenbacher K, Besser S, Hass N, Breer H. 2006b. Olfactory receptors and signalling elements in the Grueneberg ganglion. J Neurochem 98(2):543-554.

Fleischer J, Schwarzenbacher K, Breer H. 2007. Expression of trace amine-associated receptors in the Grueneberg ganglion. Chem Senses 32(6):623-631.

French PJ, Bijman J, Edixhoven M, Vaandrager AB, Scholte BJ, Lohmann SM, Nairn AC, de Jonge HR. 1995. Isotype-specific activation of cystic fibrosis transmembrane conductance regulator-chloride channels by cGMP-dependent protein kinase II. J Biol Chem 270(44):26626-26631.

Frings S, Lynch JW, Lindemann B. 1992. Properties of cyclic nucleotide-gated channels mediating olfactory transduction. Activation, selectivity, and blockage. J Gen Physiol 100(1):45-67.

Fulle HJ, Vassar R, Foster DC, Yang RB, Axel R, Garbers DL. 1995. A receptor guanylyl cyclase expressed specifically in olfactory sensory neurons. Proc Natl Acad Sci U S A 92(8):3571-3575.

Fuss B, Mallon B, Phan T, Ohlemeyer C, Kirchhoff F, Nishiyama A, Macklin WB. 2000. Purification and analysis of in vivo-differentiated oligodendrocytes expressing the green fluorescent protein. Dev Biol 218(2):259-274.

Fuss SH, Omura M, Mombaerts P. 2005. The Grueneberg ganglion of the mouse projects axons to glomeruli in the olfactory bulb. Eur J Neurosci 22(10):2649-2654.

Golin-Bisello F, Bradbury N, Ameen N. 2005. STa and cGMP stimulate CFTR translocation to the surface of villus enterocytes in rat jejunum and is regulated by protein kinase G. Am J Physiol Cell Physiol 289(3):C708-716.

Grüneberg H. 1973. A ganglion probably belonging to the N. terminalis system in the nasal mucosa of the mouse. Z Anat Entwicklungsgesch 140(1):39-52.

Halpern M. 1987. The organization and function of the vomeronasal system. Annu Rev Neurosci 10:325-362.

Henion TR, Qu Q, Smith FI. 2003. Expression of dystroglycan, fukutin and POMGnT1 during mouse cerebellar development. Brain Res Mol Brain Res 112(1-2):177-181.

Hu J, Zhong C, Ding C, Chi Q, Walz A, Mombaerts P, Matsunami H, Luo M. 2007. Detection of near-atmospheric concentrations of CO2 by an olfactory subsystem in the mouse. Science 317(5840):953-957.

Jarchau T, Hausler C, Markert T, Pohler D, Vanderkerckhove J, De Jonge HR, Lohmann SM, Walter U. 1994. Cloning, expression, and in situ localization of rat intestinal cGMP-dependent protein kinase II. Proc Natl Acad Sci U S A 91(20):9426-9430.

Juilfs DM, Fulle HJ, Zhao AZ, Houslay MD, Garbers DL, Beavo JA. 1997. A subset of olfactory neurons that selectively express cGMP-stimulated phosphodiesterase (PDE2) and guanylyl cyclase-D define a unique olfactory signal transduction pathway. Proc Natl Acad Sci U S A 94(7):3388-3395.

Kohl S, Marx T, Giddings I, Jagle H, Jacobson SG, Apfelstedt-Sylla E, Zrenner E, Sharpe LT, Wissinger B. 1998. Total colourblindness is caused by mutations in the gene encoding the alpha-subunit of the cone photoreceptor cGMP-gated cation channel. Nat Genet 19(3):257-259.

Koo JH, Gill S, Pannell LK, Menco BP, Margolis JW, Margolis FL. 2004. The interaction of Bex and OMP reveals a dimer of OMP with a short half-life. J Neurochem 90(1):102-116.

Koos DS, Fraser SE. 2005. The Grueneberg ganglion projects to the olfactory bulb. Neuroreport 16(17):1929-1932.

Kuhn M. 2003. Structure, regulation, and function of mammalian membrane guanylyl cyclase receptors, with a focus on guanylyl cyclase-A. Circ Res 93(8):700-709.

Kuhn M, Ng CK, Su YH, Kilic A, Mitko D, Bien-Ly N, Komuves LG, Yang RB. 2004. Identification of an orphan guanylate cyclase receptor selectively expressed in mouse testis. Biochem J 379(Pt 2):385-393.

Leinders-Zufall T, Cockerham RE, Michalakis S, Biel M, Garbers DL, Reed RR, Zufall F, Munger SD. 2007. Contribution of the receptor guanylyl cyclase GC-D to chemosensory function in the olfactory epithelium. Proc Natl Acad Sci U S A 104(36):14507-14512.

Macklin WB, Campagnoni CW, Deininger PL, Gardinier MV. 1987. Structure and expression of the mouse myelin proteolipid protein gene. J Neurosci Res 18(3):383-394.

Markert T, Vaandrager AB, Gambaryan S, Pohler D, Hausler C, Walter U, De Jonge HR, Jarchau T, Lohmann SM. 1995. Endogenous expression of type II cGMP-dependent protein kinase mRNA and protein in rat intestine. Implications for cystic fibrosis transmembrane conductance regulator. J Clin Invest 96(2):822-830.

Matveev AV, Quiambao AB, Browning Fitzgerald J, Ding XQ. 2008. Native cone photoreceptor cyclic nucleotide-gated channel is a heterotetrameric complex comprising both CNGA3 and CNGB3: a study using the cone-dominant retina of Nrl-/- mice. J Neurochem 106(5):2042-2055.

Meyer MR, Angele A, Kremmer E, Kaupp UB, Muller F. 2000. A cGMP-signaling pathway in a subset of olfactory sensory neurons. Proc Natl Acad Sci U S A 97(19):10595-10600.

Munger SD, Leinders-Zufall T, Zufall F. 2008. Subsystem Organization of the Mammalian Sense of Smell. Annu Rev Physiol.

Nave KA, Lai C, Bloom FE, Milner RJ. 1987. Splice site selection in the proteolipid protein (PLP) gene transcript and primary structure of the DM-20 protein of central nervous system myelin. Proc Natl Acad Sci U S A 84(16):5665-5669.

Papastefanaki F, Chen J, Lavdas AA, Thomaidou D, Schachner M, Matsas R. 2007. Grafts of Schwann cells engineered to express PSA-NCAM promote functional recovery after spinal cord injury. Brain 130(Pt 8):2159-2174.

Potter SM, Wang CM, Garrity PA, Fraser SE. 1996. Intravital imaging of green fluorescent protein using two-photon laser-scanning microscopy. Gene 173(1 Spec No):25-31.

Potter SM, Zheng C, Koos DS, Feinstein P, Fraser SE, Mombaerts P. 2001. Structure and emergence of specific olfactory glomeruli in the mouse. J Neurosci 21(24):9713-9723.

Rena G, Begg F, Ross A, MacKenzie C, McPhee I, Campbell L, Huston E, Sullivan M, Houslay MD. 2001. Molecular cloning, genomic positioning, promoter identification, and characterization of the novel cyclic amp-specific phosphodiesterase PDE4A10. Mol Pharmacol 59(5):996-1011.

Ring G, Mezza RC, Schwob JE. 1997. Immunohistochemical identification of discrete subsets of rat olfactory neurons and the glomeruli that they innervate. J Comp Neurol 388(3):415-434.

Roppolo D, Ribaud V, Jungo VP, Luscher C, Rodriguez I. 2006. Projection of the Gruneberg ganglion to the mouse olfactory bulb. Eur J Neurosci 23(11):2887-2894.

Sadhu K, Hensley K, Florio VA, Wolda SL. 1999. Differential expression of the cyclic GMP-stimulated phosphodiesterase PDE2A in human venous and capillary endothelial cells. J Histochem Cytochem 47(7):895-906.

Scheving LA, Russell WE. 1996. Guanylyl cyclase C is up-regulated by nonparenchymal cells and hepatocytes in regenerating rat liver. Cancer Res 56(22):5186-5191.

Scheving LA, Russell WE, Chong KM. 1996. Structure, glycosylation, and localization of rat intestinal guanylyl cyclase C: modulation by fasting. Am J Physiol 271(6 Pt 1):G959-968.

Schulz S, Wedel BJ, Matthews A, Garbers DL. 1998. The cloning and expression of a new guanylyl cyclase orphan receptor. J Biol Chem 273(2):1032-1037.

Shakur Y, Wilson M, Pooley L, Lobban M, Griffiths SL, Campbell AM, Beattie J, Daly C, Houslay MD. 1995. Identification and characterization of the type-IVA cyclic AMP-specific phosphodiesterase RD1 as a membrane-bound protein expressed in cerebellum. Biochem J 306 (Pt 3):801-809.

Shinoda K, Ohtsuki T, Nagano M, Okumura T. 1993. A possible functional necklace formed by placental antigen X-P2-immunoreactive and intensely acetylcholinesterase-reactive (PAX/IAE) glomerular complexes in the rat olfactory bulb. Brain Res 618(1):160-166.

Shinoda K, Shiotani Y, Osawa Y. 1989. "Necklace olfactory glomeruli" form unique components of the rat primary olfactory system. J Comp Neurol 284(3):362-373.

Sokal I, Alekseev A, Palczewski K. 2003. Photoreceptor guanylate cyclase variants: cGMP production under control. Acta Biochim Pol 50(4):1075-1095.

Storan MJ, Key B. 2006. Septal organ of Gruneberg is part of the olfactory system. J Comp Neurol 494(5):834-844.

Stowers L, Holy TE, Meister M, Dulac C, Koentges G. 2002. Loss of sex discrimination and male-male aggression in mice deficient for TRP2. Science 295(5559):1493-1500.

Sun L, Wang H, Hu J, Han J, Matsunami H, Luo M. 2009. Guanylyl cyclase-D in the olfactory CO2 neurons is activated by bicarbonate. Proc Natl Acad Sci U S A 106(6):2041-2046.

Tachibana T, Fujiwara N, Nawa T. 1990. The ultrastructure of the ganglionated nerve plexus in the nasal vestibular mucosa of the musk shrew (Suncus murinus, insectivora). Arch Histol Cytol 53(2):147-156.

Tanaka JC, Eccleston JF, Furman RE. 1989. Photoreceptor channel activation by nucleotide derivatives. Biochemistry 28(7):2776-2784.

Trinh K, Storm DR. 2003. Vomeronasal organ detects odorants in absence of signaling through main olfactory epithelium. Nat Neurosci 6(5):519-525.

Verhagen JV, Wesson DW, Netoff TI, White JA, Wachowiak M. 2007. Sniffing controls an adaptive filter of sensory input to the olfactory bulb. Nat Neurosci 10(5):631-639.

Walz A, Feinstein P, Khan M, Mombaerts P. 2007. Axonal wiring of guanylate cyclase-D-expressing olfactory neurons is dependent on neuropilin 2 and semaphorin 3F. Development 134(22):4063-4072.

Wight PA, Duchala CS, Readhead C, Macklin WB. 1993. A myelin proteolipid protein-LacZ fusion protein is developmentally regulated and targeted to the myelin membrane in transgenic mice. J Cell Biol 123(2):443-454.

TABLES

Table 1: Antibodies used in this study

Antibody	Vendor	Dilution	Immunizing Sequence	Mouse Homology
Goat anti-OMP (whole antiserum)	Wako #54-1000	1:13,000	Rat OMP (NP_036748) 1-163	163/163 (100%)
Rabbit anti-Pde2a (affinity-purified)	Fabgennix #PD2A-101AP	1:1,000	Rat Pde2a (NP_001137319) 904-921 SNNSLDFLDEEYEVPDLD	18/18 (100%)
Rabbit anti-Pde4a (affinity-purified)	Fabgennix #PD4-112AP	1:250	Rat Pde4a (NP_037233) 831-844 ISAPGRWGSGGDPA	14/14 (100%)
Rabbit anti-cGKII (whole antiserum)	Santa Cruz Biotechnology # sc-25430	1:200	Human cGKII (NP_006250) 1-120	108/120 (90%)
Rabbit anti-CNGA3 (whole antiserum)	Kindly provided by X.-Q. Ding	1:750	Mouse CNGA3 (NP_034048) 77-97 SNAQPNPGEQKPPDGGEGRKE	21/21 (100%)
Rabbit anti-pGC-A (affinity-purified)	Fabgennix #PGCA-101AP	1:250	Rat pGC-A (NP_036745) 1042-1057 VRTYWLLGERGCSTRG	16/16 (100%)
Rabbit anti-pGC-B (affinity-purified)	Fabgennix #PGCB-201AP	1:200	Rat pGC-B (NP_446290) 1029-1047 GKMRTYWLLGERKGPPGLL	18/19 (95%)
Rabbit anti-pGC-C (affinity-purified)	Fabgennix #PGCC-301AP	1:200	Rat pGC-C (NP_037302) 1048-1063 RVASYKKGFLEYMQLN	16/16 (100%)
Rabbit anti-pGC-E (affinity-purified)	Fabgennix #PGCE-501AP	1:1,000	Rat pGC-E (NP_077356) 1091-1108 PERRKKLEKARPGQFTGK	18/18 (100%)
Rabbit anti-pGC-F (affinity-purified)	Fabgennix #PGCF-601AP	1:400	Rat pGC-F (NP_446283) 1090-1108 EIAAFQRRKAERQLVRNKP	19/19 (100%)
Rabbit anti-pGC-G (affinity-purified)	Fabgennix #PGCG-701AP	1:500	Rat pGC-G (NP_620611) 1085-1100 PLPEFTEEEAKVPEIL	15/16 (94%)
Rabbit anti-GFAP (whole antiserum)	Abcam # ab7260	1:600	Human GFAP (NP_002046) 1-432	393/432 (91%)
Rabbit anti-PLP (whole antiserum)	Abcam # ab28486	1:500	Mouse myelin PLP (NP_035253) 109-128 CGKGLSATVTGGQKGRGSRG	20/20 (100%)

Described are the host animals, commercial sources, working concentrations, and immunizing sequences (with accession numbers) of the antibodies.

Table 2: Western blot characterization of pGC antibodies

Antibody	Mouse Tissue Lysate	Approximate Detected Bands (kDa)	Predicted Band (kDa)
Rabbit anti-pGC-A	Kidney	120	119
Rabbit anti-pGC-B	Kidney	120	117
Rabbit anti-pGC-C	Intestine	180, 55	120*
Rabbit anti-pGC-E	Retina	110	120
Rabbit anti-pGC-F	Retina	110	124
Rabbit anti-pGC-G	Nasal vestibule	120	123

* Observed band size for pGC-C on immunoblots is known to be variable, ranging from 50 to 240 kDa (Scheving and Russell, 1996; Scheving et al., 1996).

Described are the results of immunoblots performed with pGC antibodies on various mouse tissue sources.

FIGURE LEGENDS

Figure 1: The Grueneberg Ganglion (GG) is an unusual olfactory nerve at the rostral tip of the mouse nose. A) Schematic of the nasal cavity and septum of a mouse showing the olfactory subsystems. Both GG and GC-D subsystems (neurons as orange spots) project axons (orange lines) to a unique spatial domain containing sets of interconnected glomeruli in the caudal region of the olfactory bulb. The MOE is part of the MOS. The VNO is part of the AOS. Green lines demarcate anatomical locations in the nasal cavity; blue lines demarcate regions of the brain. B) In this medial view of a whole-mount preparation from an OMP-GFP mouse, GG neurons express olfactory marker protein (OMP, in white) and are arranged as clusters of cells comprising an arrowhead-shaped organ. C) OMP-expressing GG neurons (green) seen in thin section do not project cellular processes into the nasal cavity (n.c.). They are separated by a keratinized epithelium (KE, magenta) that is labeled with an antibody to particulate guanylate cyclase E. D) *En face* view of proteolipid protein (PLP-GFP)-expressing glial cells in the nasal vestibule that ensheathe GG neurons. In thin sections (E-G): E) GG neurons visualized in nasal vestibules of OMP-GFP mice (GFP in green) positively stain for OMP protein (magenta). F) GFP-positive OSNs (green) in the OMP-GFP mouse MOE stain positively for OMP (magenta). G) OMP-GFP mice faithfully report expression of OMP in the glomerular layer (GL) of the olfactory bulb (GFP in green, OMP immunostaining in magenta). SO = septal organ; D = dorsal; V = ventral; R = rostral; C = caudal; ONL = olfactory nerve layer; EPL = external plexiform layer. Scale bars: B) 250 μm; C) 15 μm; D) 60 μm; E-F) 30 μm; G) 60 μm.

Figure 2: The GG expresses a cGMP-stimulated phosphodiesterase. A-B) PDE4A staining in thick sections from neonatal OMP-GFP mice in the MOE (A) and the rostral nasal vestibule (B). GG neurons correspond to OMP-positive cells in the nasal vestibule. C-D) PDE2A staining in the neonatal MOE (C) and nasal vestibule (D). The PDE2A antibody labeled GG neurons and vascular endothelial cells in the nasal vestibule. E-F) Immunoadsorption study with the PDE2A antibody in whole-mount preparations. Unblocked PDE2A antibody (magenta) labeled adult GG neurons (green) in the nasal vestibules of OMP-

GFP mice (E), but there was no labeling when the antibody was blocked with the immunizing peptide (F). Scale bars: 40 μm.

Figure 3: Downstream cGMP signal transduction components are expressed in the GG. A) In OMP-GFP mice, GFP-fluorescing GG neurons (green) in the nasal vestibule express cGKII (magenta). On some neurons the cGKII antibody labels the GG neuron membrane (arrow). B) The cGKII antibody (red) labels the villus brush borders in the intestine (nuclei are in blue). C) CNGA3 antibody (red) labels photoreceptor segments (arrow) in thin sections from the mouse retina (nuclei are in blue). D) GG neurons (green) express CNGA3 (magenta) on unusual "whip-like" subcellular domains. E) Neurons of the GC-D olfactory subsystem, highlighted by GFP expression (green) in the GCD-iTG transgenic mouse, express CNGA3 (magenta) on their dendritic knobs (arrows). Scale bars: A) 20 μm B) 60 μm; C) 30 μm; D) 20 μm; E) 60 μm.

Figure 4: The GG does not express pGC-D. A) PDE2A immunolabeling in thick sections from the olfactory neuroepithelium of a transgenic GCD-iTG mouse. GFP-positive GC-D neurons (green) express PDE2A (magenta), consistent with their use of a cGMP signaling pathway. B) PDE2A-positive GG cells (magenta) in thick sections from the nasal vestibule are devoid of GFP (green) and, hence, pGC-D. Scale bars: 60 μm.

Figure 5: Particulate guanylate cyclase expression in the GG. A-B) In whole-mount preparations, all GG neurons (green) express pGC-G (A, magenta) on unusual subcellular domains. In contrast, only a small, broadly distributed subset of GG neurons (white asterisks) express pGC-A (B, magenta) on the same subcellular domains. C-D) Immunoadsorption study with the pGC-G antibody (magenta) and its antigenic blocking peptide on GG neurons (green). Labeling is observed when the antibody is unblocked (C) but is abolished when it is blocked (D). E-F) Blocking experiment with the pGC-A antibody (magenta) on GG neurons (green). Unblocked antibody labels the small GG neuron subset (E), blocked antibody does not

(F). G-H) pGC-G is expressed in GG neurons (red asterisks) at all ages, from PD2/neonatal (G) to adult (H) ages. Gray-black areas indicate staining. I-J) A comparison on pGC-G expression the GG and GC-D olfactory subsystems of GCD-iTG mice reveals that pGC-G (magenta) is expressed in GG neurons of the nasal vestibule (I) but not in the GC-D neurons (green) of the caudal MOE (J). K) High magnification view of pGC-G-expressing "whip"-like subcellular domains (black staining, red arrows) in a whole-mount preparation. L) High magnification view of pGC-G localization (magenta) on a GG neuron (green) at different optical z planes (in μm) in thin sections. Labeled subcellular domains follow the surface contours of GG neurons. M) Immunoblot with pGC-G antibody on nasal vestibule lysate. A single 120 kDa band is labeled. Lanes correspond to the relative amount of protein loaded. Scale bars: A-B) 60 μm; C-F) 10 μm; G-H) 40 μm; I-J) 30 μm; K) 15 μm; L) 5 μm.

Figure 6: pGC-G expression in relation to the GG ensheathing cells. A) In whole-mount preparations, GFP-positive fibers (green) in the nasal vestibules of PLP-GFP mice colocalize with GFAP staining (magenta). B) In thin cross sections of the nasal vestibule, GFP-positive cells (green) in PLP-GFP mice can be seen to envelop GG neurons stained with the OMP antibody (magenta). C) In thin sections, pGC-G (magenta) does not colocalize with the glial-like ensheathing cell population (green) visualized in PLP-GFP mice. Scale bars: A) 25 μm; B-C) 20 μm.

Figure 7: Ultrastructural view of GG neurons. A) Low magnification view of a single GG neuron. A cluster of ciliary basal bodies is visible in the yellow highlighted region, next to the nucleus [1]. The GG neuron is ensheathed by a glial cell [2]. B) The inset region of (A), magnified. Ciliary basal bodies [3] are in close proximity to a mitochondrion [4]. C-D) A closer view of the clusters of ciliary basal bodies [3]. These clusters are supported by a ring of actin filaments, visible in (D). E-F) Out of these basal bodies, long ciliary fibers [5] erupt and follow the membrane contour of the GG neuron. These fibers are held tight to the membrane by the glial-like ensheathing cells. Lower-right orange inset magnified areas outlined in red (F). Scale bars: A) 3 μm; B) 0.5 μm; C-D) 0.25 μm; E) 0.5 μm F) 1 μm (inset: 0.3 μm).

Figure 8: The cGMP signal transduction pathway in the GG. Binding of atrial natriuretic peptide (ANP), B-type natriuretic peptide (BNP), or other as-of-yet unidentified ligands to pGC-A or unknown ligands to pGC-G induces the conversion of GTP to cGMP by the particulate guanylate cyclases. The produced cGMP can then open CNGA3 channels to depolarize the GG neuron, induce additional signaling through cGKII, or be degraded to GMP by PDE2A.

ABBREVIATIONS

ANP	Atrial natriuretic peptide
AOS	Accessory Olfactory System
BNP	B-type natriuretic peptide
cGKII	cGMP-dependent kinase II
cGMP	Cyclic guanosine monophosphate
CNGA3	Cyclic nucleotide gated channel A3
EPL	External plexiform layer
GC-D	Particulate guanylate cyclase D
GFAP	Glial fibrillary acidic protein
GFP	Green fluorescent protein
GG	Grueneberg Ganglion
GMP	Guanosine monophosphate
GTP	Guanosine triphosphate
iTG	Internal ribosome entry site fused to tau protein fused to GFP
iTL	Internal ribosome entry site fused to tau protein fused to LacZ
MOE	Main Olfactory Epithelium
MOS	Main Olfactory System
n.c.	Nasal cavity
OMP	Olfactory marker protein
ONL	Olfactory nerve layer
OSN	Olfactory sensory neuron
PDE2A	Phosphodiesterase 2a
PDE4A	Phosphodiesterase 4a
pGC-A	Particulate guanylate cyclase A
pGC-D	Particulate guanylate cyclase D
pGC-G	Particulate guanylate cyclase G
PLP	Proteolipid protein
SO	Septal organ
TEM	Transmission electron microscopy
tg	Transgenic animal
VNO	Vomeronasal Organ

FIGURES

Figure 1:

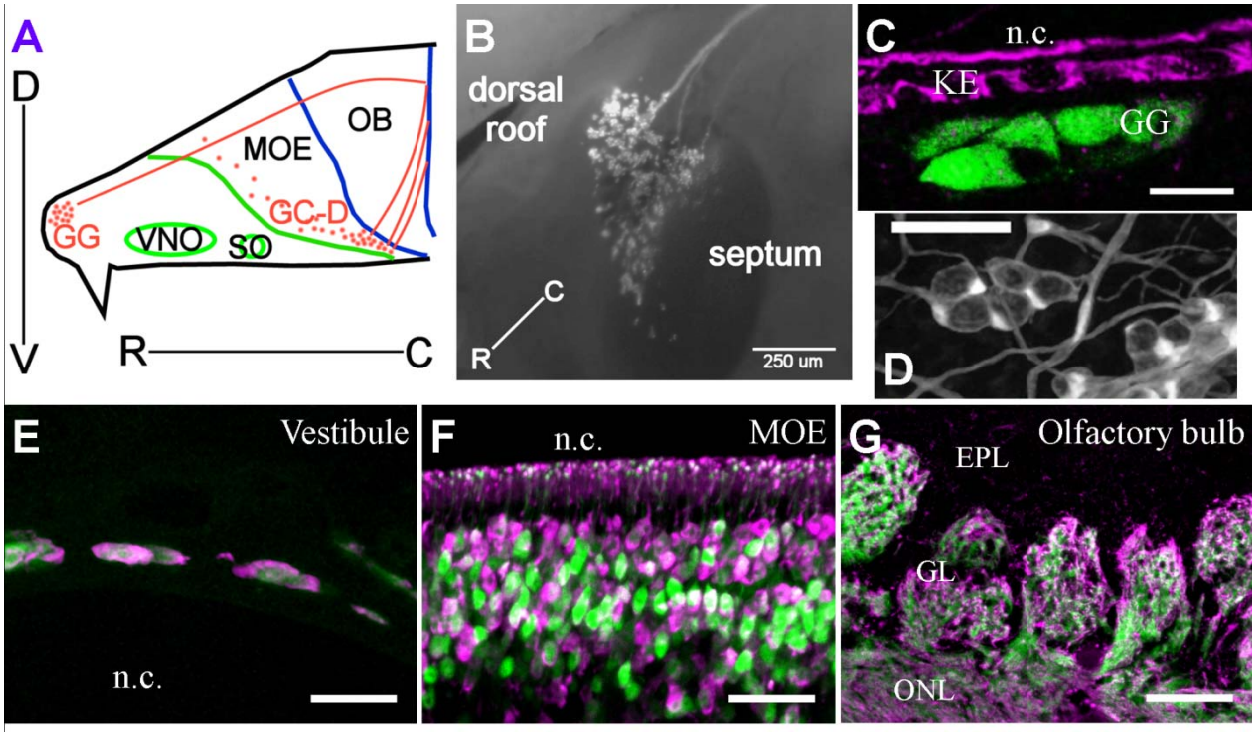

Figure 2:

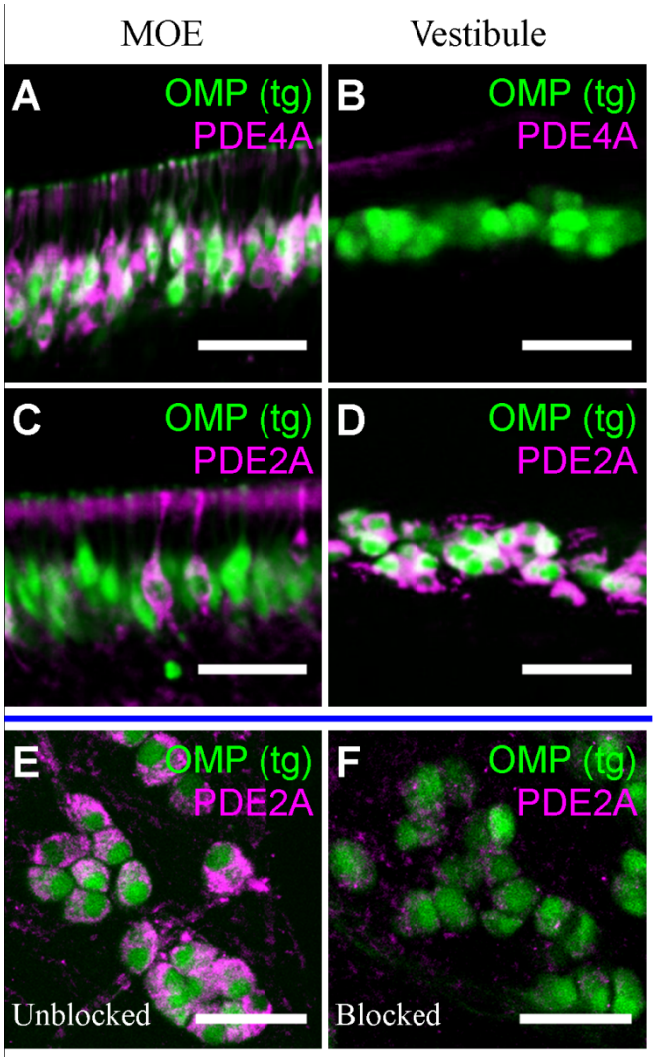
MOE
Vestibule
A
OMP (tg)
PDE4A
B
OMP (tg)
PDE4A
C
OMP (tg)
PDE2A
D
OMP (tg)
PDE2A
E
OMP (tg)
PDE2A
Unblocked
F
OMP (tg)
PDE2A
Blocked

Figure 3:

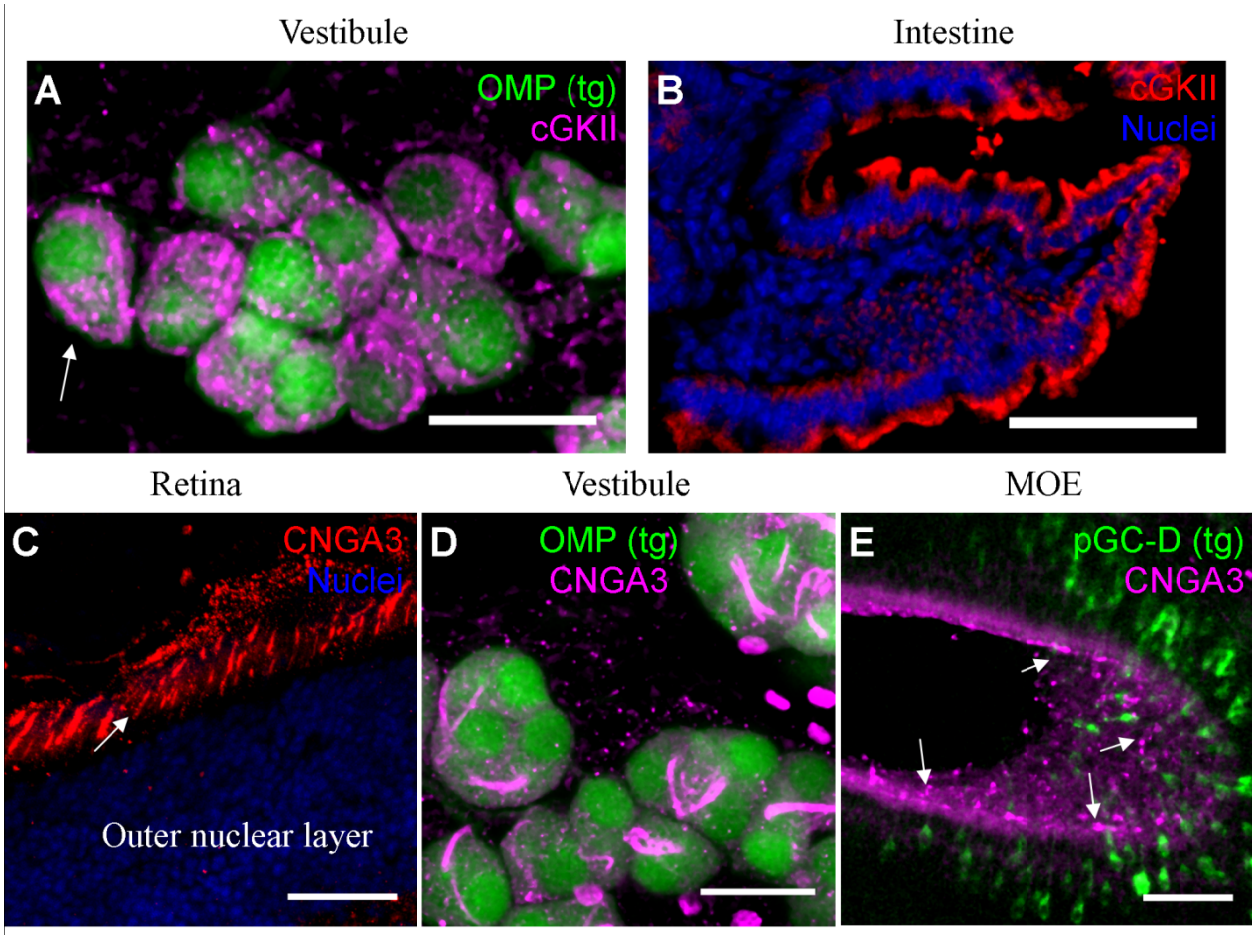
Vestibule
Intestine
A
OMP (tg)
cGKII
B
cGKII
Nuclei
Retina
Vestibule
MOE
C
CNGA3
Nuclei
Outer nuclear layer
D
OMP (tg)
CNGA3
E
pGC-D (tg)
CNGA3

Figure 4:

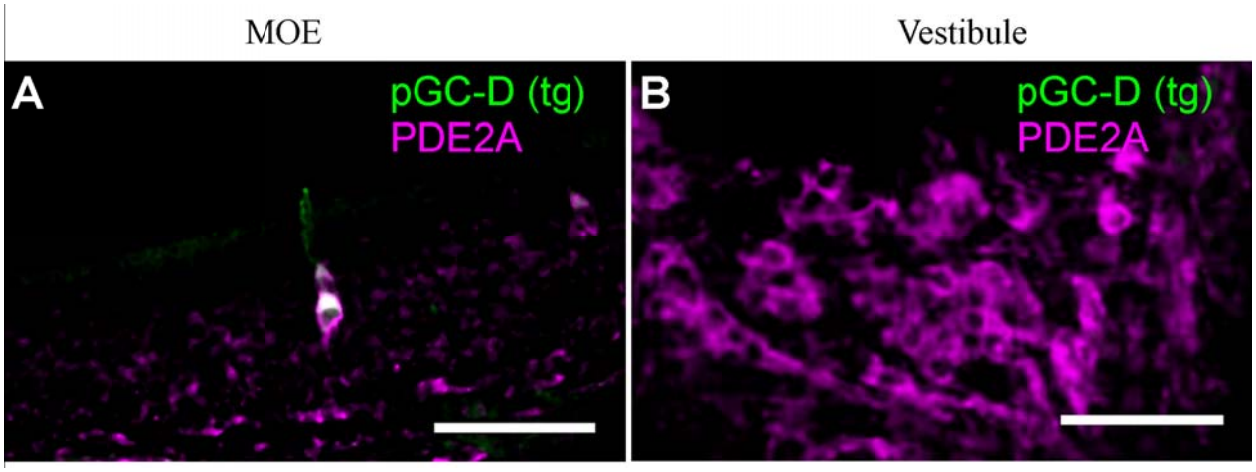

Figure 5:

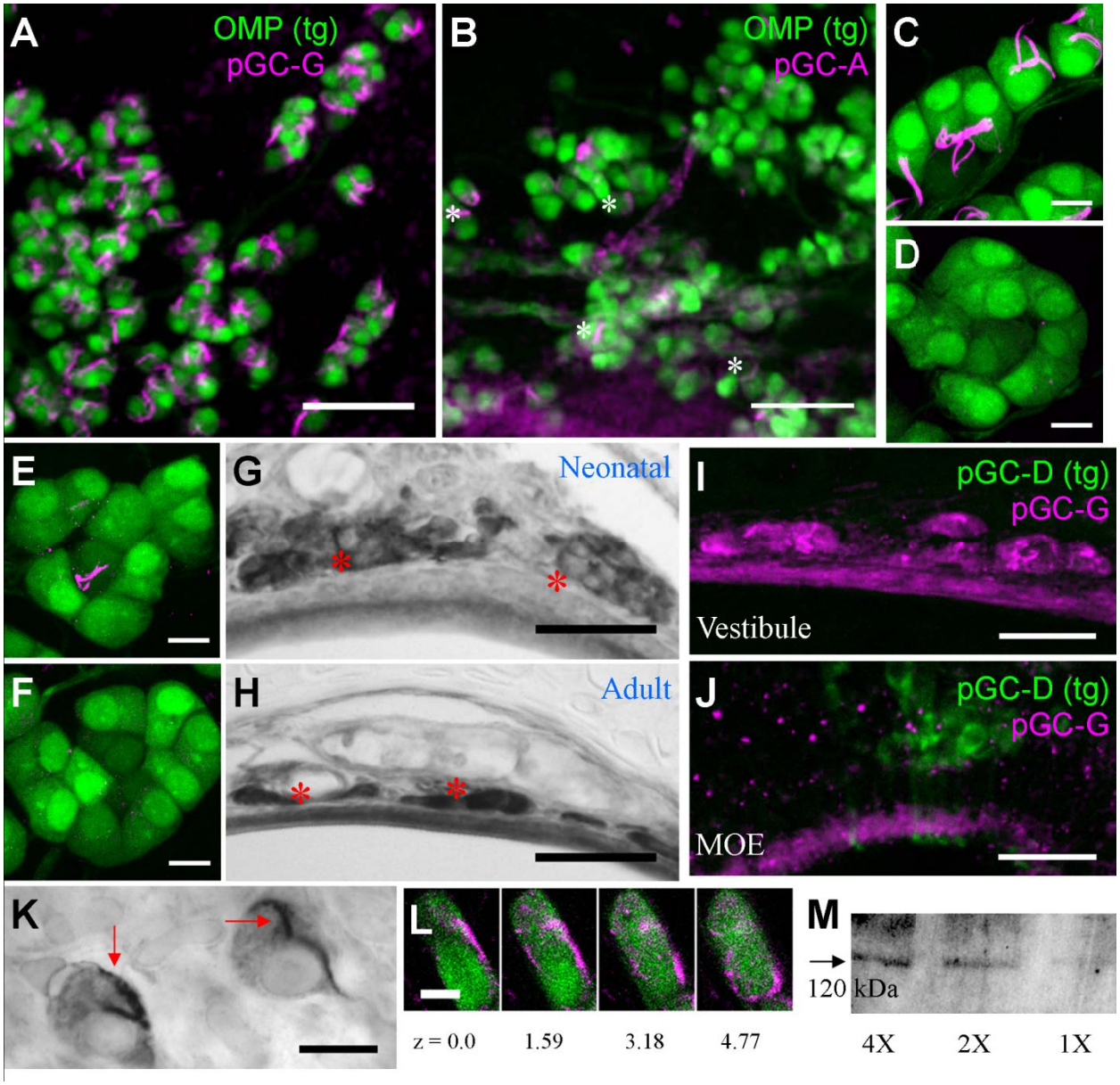
A
OMP (tg)
pGC-G
B
OMP (tg)
pGC-A
C
D
E
F
G
Neonatal
H
Adult
I
pGC-D (tg)
pGC-G
Vestibule
J
pGC-D (tg)
pGC-G
MOE
K
L
z = 0.0
1.59
3.18
4.77
M
120 kDa
4X
2X
1X

Figure 6:

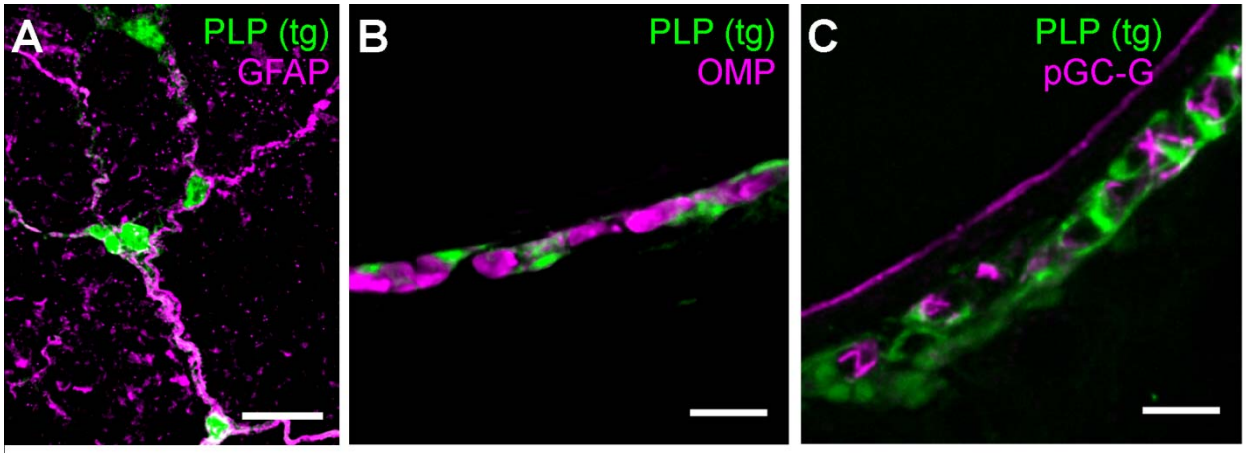

Figure 7:

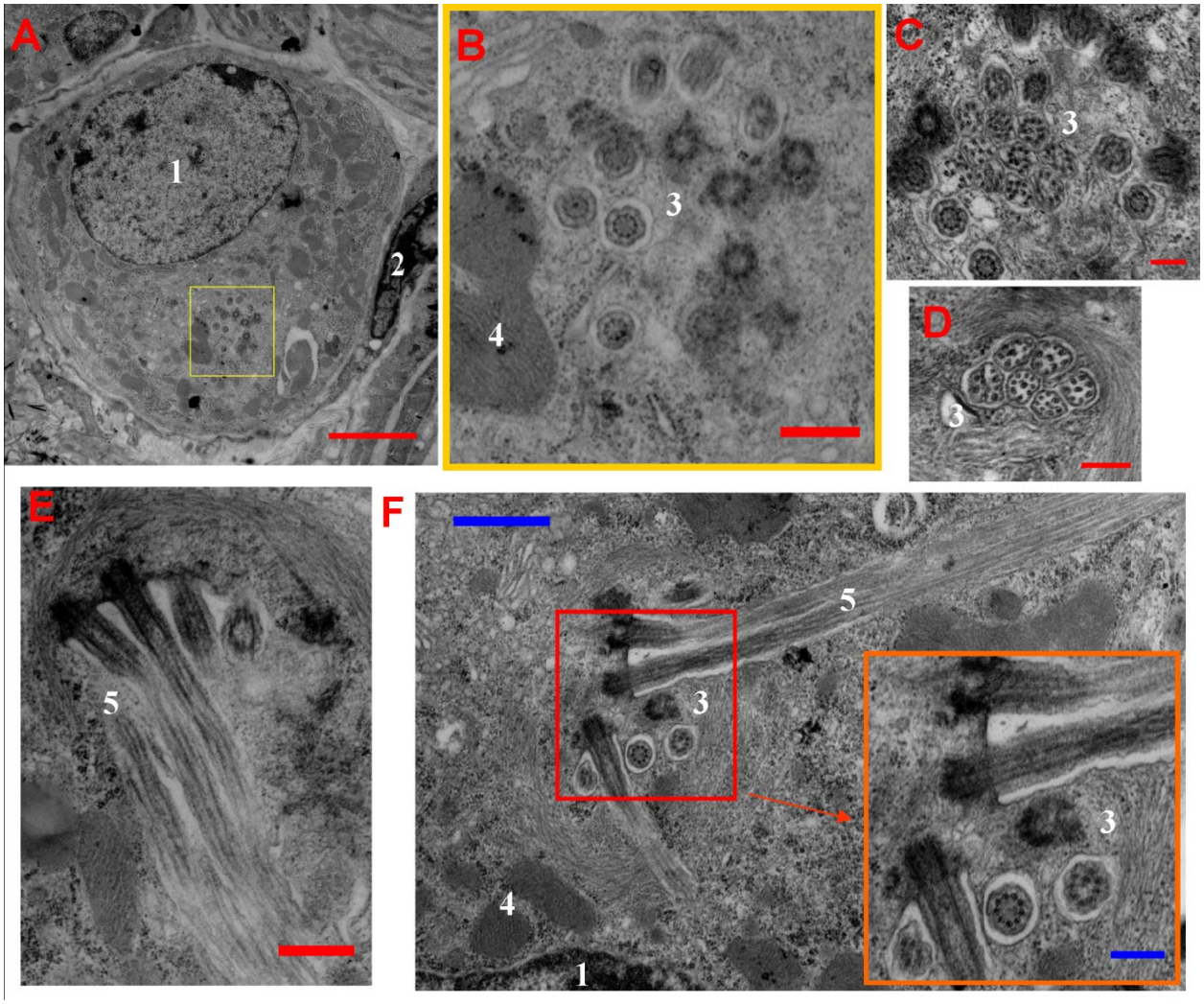

Figure 8:

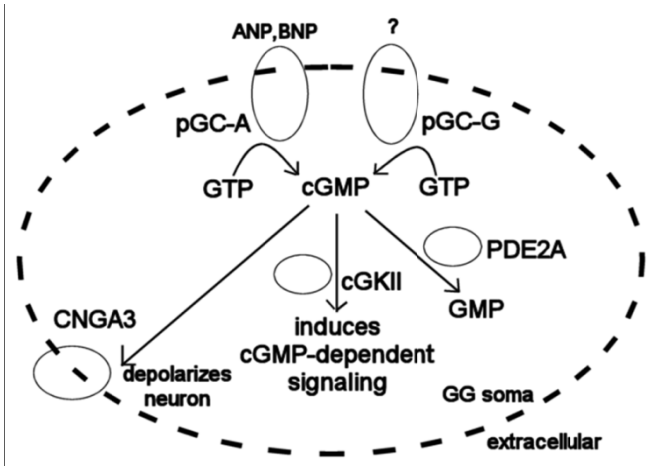
ANP,BNP
?
pGC-A
pGC-G
GTP
cGMP
GTP
PDE2A
cGKII
GMP
CNGA3
induces
cGMP-dependent
signaling
depolarizes
neuron
GG soma
extracellular

SUPPORTING FIGURES

Supporting Figure 1:

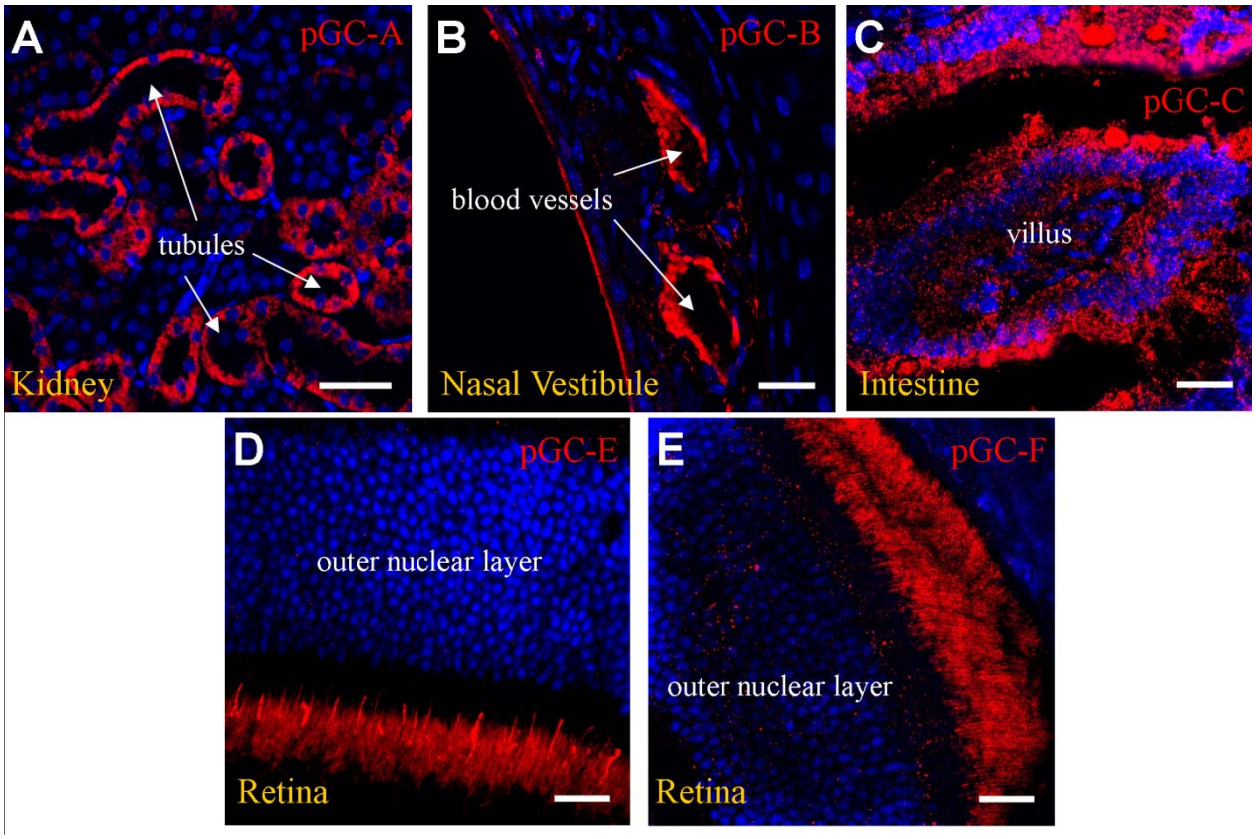

Immunohistochemical validation of pGC antibodies on different tissue types. Antibodies to pGC-A (A), pGC-B (B), pGC-C (C), pGC-E (D), and pGC-F (E) were used to stain kidney (A), nose (B), intestine (C), and retinal (D,E) tissue. Antibody signal is in red. Nuclei visualized using Topro-3 are in blue. These antibodies each exuberantly recognized proteins in their respective control tissues. Thus, they are fit for use in immunostaining experiments. Scale bars: A) 40 µm; B-E) 20 µm.